JULY 08 2020

Field measurements of acoustic absorption in seawater from 38 to 360 kHz

Gavin J. Macaulay ; Dezhang Chu ; Egil Ona

J Acoust Soc Am 148, 100–107 (2020)
https://doi.org/10.1121/10.0001498

JASA ARTICLE

Field measurements of acoustic absorption in seawater from 38 to 360 kHz

Gavin J. Macaulay,[1,a)] Dezhang Chu,[2,b)] and Egil Ona[1]

[1]*Marine Ecosystem Acoustics, Institute of Marine Research, Nykirkekaien 1, Bergen, 5004, Norway*

[2]*Northwest Fisheries Science Center, National Marine Fisheries Service, National Oceanic and Atmospheric Administration, 2725 Montlake Boulevard East, Seattle, Washington 98112, USA*

ABSTRACT:

Accurate estimates of acoustic absorption in seawater are crucial to the acoustic estimation of aquatic biomass. Estimates of acoustic absorption were obtained via a "pulse-echo" method, implemented using commonly available scientific echosounders and spherical calibration targets over a range of discrete frequencies. Below about 200 kHz, the absorption estimates were not significantly different from those of existing formulas, but at around 333 kHz, the measured absorption was 15 dB km^{-1} higher than estimated from existing formulas. Measurement variability was about ± 2 dB km^{-1} for all frequencies. This is consistent with an observed anomaly between modelled and measured frequency-dependent biological backscatter. Allowing for this deviation will avoid incorrect spectral-based classification of acoustic targets and improve uncertainty in aquatic biomass estimation.

 https://doi.org/10.1121/10.0001498

(Received 12 November 2019; revised 9 June 2020; accepted 11 June 2020; published online 8 July 2020)

[Editor: Timothy Duda] Pages: 100–107

I. INTRODUCTION

In this work, experimental and processing procedures are presented that enable the estimation of acoustic absorption in the water between an echosounder and a known target. This is applied at frequencies between 38 and 360 kHz. The results are consistent with anecdotal observations that commonly used absorption equations are not accurate for some water properties in the frequency band around 333 kHz. Potential causes of this inaccuracy are discussed.

The use of active acoustic techniques to estimate the biomass of fish populations requires accurate estimates of the backscatter from those populations. Any error in the backscatter leads directly to an error in biomass estimates and, via the stock assessment process, could affect fishing resource management and the sustainability of fish populations. Quantitative backscatter measurement requires a compensation for absorption of acoustic energy by water and, because most acoustically surveyed fish populations are found in marine waters, the absorption in seawater is of particular interest.

Acoustic absorption in seawater is comprised of three components: absorption by pure water, absorption by boric acid, and absorption by salts of magnesium (Francois and Garrison, 1982a). The boric acid contribution is only significant at frequencies below 10 kHz, whereas the pure water contribution is dominant above 1 MHz. The magnesium salt contribution (almost entirely due to magnesium sulphate) is significant at the typical operating frequencies of echosounders used to measure fisheries' biomass (12–500 kHz).

A survey-specific estimate of acoustic absorption is typically derived from water property measurements that serve as input to established relationships. These relationships have been obtained from multiple measurements of absorption over a range of water properties, including both *in situ* and laboratory-based resonator measurements using either natural or artificial seawater. Such experiments were first conducted in the 1940s (Liebermann, 1948), continuing through to the 1980s, in which the relationship commonly used today was presented (Francois and Garrison, 1982b, 1982a). More recent work has focused on alternative and, perhaps, improved derivations of relationships from the same datasets (Ainslie and McColm, 1998; Doonan *et al.*, 2003; van Moll *et al.*, 2009) and additional spot measurements that agree with the Francois and Garrison equation (Ochi *et al.*, 2009). However, the individual measurements that have been used to generate these relationships contain considerable variability and show bias at some parameter values. For example, of the 25 measurements between 250 and 350 kHz that contributed to the estimate of the magnesium sulphate relaxation frequency (Table II and Fig. 9 in Francois and Garrison, 1982b), 23 were higher than the final absorption relationship (range was -2.4–19.8 dB km^{-1}). In addition, for some parameter ranges, the sensitivity to the parameters is relatively high—for example, at a salinity of 35 PSU, the absorption equations are particularly sensitive to temperature for frequencies between about 70 and 200 kHz (Fig. 8 of Francois and Garrison, 1982a). The measurements used to derive the pure water contribution (compiled by Kurtze and Tamm, 1953) also show considerable

a)Electronic mail: gavin@macaulay.co.nz, ORCID:0000-0003-2518-6537.
b)ORCID:0000-0001-5196-4991.

https://doi.org/10.1121/10.0001498

scatter around the fitted relationship of Francois and Garrison (1982b).

The error in fisheries biomass estimates caused by an incorrect absorption increases with range between the acoustic transducer and the fish of interest. For most acoustic frequencies used in fisheries acoustics applications, ranges are sufficiently short that even moderate errors in the estimated absorption (for example, 2–3 dB km^{-1}) have a minimal effect on the biomass estimate. In addition, errors resulting from inaccurate absorption estimates are typically much smaller than those caused by the many other sources of bias and uncertainty in acoustic biomass estimates (Doonan *et al.*, 2003).

However, for applications involving longer ranges or higher frequencies, these errors can cause a significant bias. For example, in acoustic surveys of smooth oreos (*Pseudocyttus maculatus*) at 38 kHz, in which the acoustic return-travel distances are up to 1800 m, the use of different absorption equation estimates (Francois and Garrison, 1982a, and Fisher and Simmonds, 1977) resulted in a 17% reduction or 45% increase in biomass estimates (Doonan *et al.*, 2003, in particular Fig. 5). In addition, the use of the relative frequency response to categorise the backscatter from marine organisms (Korneliussen *et al.*, 2009), combined with the development of acoustic scattering models of the same organisms, has shown an unexpected depth-dependent anomaly for Antarctic krill (*Euphausia superba*) and sandeel (*Ammodytes marinus*) at 333 kHz (Korneliussen and Johnsen, 2015), which could be explained by an incorrect absorption value.

This paper is organized as follows. In Sec. II, an experimental method (Sec. II A) and processing scheme (Secs. II B and II C) are described for estimating acoustic absorption using an echosounder and known target placed at varying ranges. Section III presents experimental measurements and processed results, which are then discussed and summarized in Sec. IV.

II. METHODS

A. Apparatus and data collection

Acoustic absorption was estimated from field experiments using a "radar pulse" method (Pinkerton, 1947) or "pulse-echo" method (Krautkrämer and Krautkrämer, 1990), in which a mono-static echosounder generates an acoustic pulse that travels through a known volume of water, reflects off a target of known scattering properties, and is then received by the same echosounder. The range to the target was progressively increased and, assuming that the water properties were sufficiently characterized and the scattering characteristics of the target were always known, an estimate of the change in absorption with range could be derived and compared to those obtained from existing equations. The target was a sphere comprised of tungsten carbide with 6% cobalt binder. The size of the sphere varied between experiments (Table I).

For the experiments presented here, the April 2012 data were collected with a Simrad EK60 split-beam narrowband scientific echosounder (Horten, Norway), and all other data were collected with a Simrad EK80 broadband split-beam scientific echosounder, operating either with narrowband pulses or frequency-modulated pulses (linear upsweep chirps).

Two operational configurations were used:

(a) The echosounder transceivers and downward-looking transducers were mounted on a cabled metal frame (the "probe") that was deployed from research vessel (RV) G. O. Sars at a fixed depth of approximately 10

TABLE I. Date, location, equipment configurations used, and water properties for each experiment. CW (continuous wave) indicates that a single frequency signal was used at the specified frequency, whereas FM (frequency modulation) indicates that a linear upsweep chirp signal was used.

Date		17 Nov. 2012	23 Apr. 2012	16 Nov. 2013	2 Nov. 2014
Time period (UTC)		17:26–18:50	15:46–17:35	12:10–15:00	17:30–18:06
Location name		Børøyfjorden	Sandviksflaket	Ullsfjorden	Bjørnafjorden
Location longitude		14° 47.96′ E	5° 19.01′ E	19° 54.22′ E	5° 28.01′ E
Location latitude		68° 51.63′ N	60° 24.51′ N	69° 57.17′ N	60° 5.88′ N
Wind (Beaufort number)		3	Not recorded	5	3
Vessel		RV G. O. Sars	FV Brennholm	RV G. O. Sars	RV G. O. Sars
Apparatus		Probe	Ship	Probe	Probe
Sphere diameter (mm)		22.0, 38.1	22.0, 38.1	21.0, 38.1	64.0
Frequency coverage (kHz)	38			CW FM (36–40)	
	70	CW			
	120	CW		CW FM (118–122)	
	200	CW	CW	CW FM (180–220)	FM
	333	CW	CW	CW FM (300–360)	FM
Average sound speed (m/s)		1480.0	1483.1	1479.8	1496.4
Average temperature (°C)		7.7	8.2	7.5	12.6

m [Fig. 1(a)]. The sphere was suspended below the frame with three monofilament lines in an inverted tripod arrangement. The sphere range could be controlled by varying the lengths of the monofilament lines. The transducers were mounted on a plate with controllable pitch and roll. At each measurement depth, the transducer plate orientation was adjusted to place the sphere within 0.2° of the center of the acoustic beam using the split-beam capability of the echosounder. Limiting the target to within 0.2° of the center minimized the uncertainty in the beampattern corrected target strength (TS), as well as avoided measurement errors due to ray bending from any layer stratification (our experiments were conducted typically above the dominant thermocline).

(b) The echosounder transceivers were installed on fishing vessel (FV) Brennholm with the downward-looking transducers mounted in a retractable keel on the hull of the vessel [Fig. 1(b)]. The sphere location and depth were controlled in a similar manner as for configuration Fig. 1(a), except that at each measurement depth, the relative lengths of the monofilament lines were adjusted to move the sphere into the center of the acoustic beam.

The procedure for each experiment involved the initial setup of the configuration, including the elimination of small bubbles on the sphere, suspension lines, and transducer (for the probe configuration) by applying a wetting agent (20:1 solution of water and liquid soap). The sphere was then placed about 10 m below the transducer, centered in the acoustic beam, and at least 100 echoes from the sphere were recorded, whereupon the range was increased and the measurement was repeated. This continued until the sphere was at such a range that the signal-to-noise ratio (SNR) went below about 10 dB (as the noise level increased, the variability in the split-beam position estimates increased, making accurate positioning of the sphere in the acoustic beam difficult, as well as increasing the variability of the sphere backscatter amplitude). The range to the sphere was then progressively decreased and further data were collected until the sphere was again about 10 m from the transducer. Measurements were performed in years 2012–2014 in various sheltered fjords along the western coastline of Norway (Table I). The range to the sphere varied from 10 to 70 m and the frequency varied from 38 to 360 kHz via five separate transducers, each with a half-power beamwidth of approximately 7° at their nominal operating frequency (Table I).

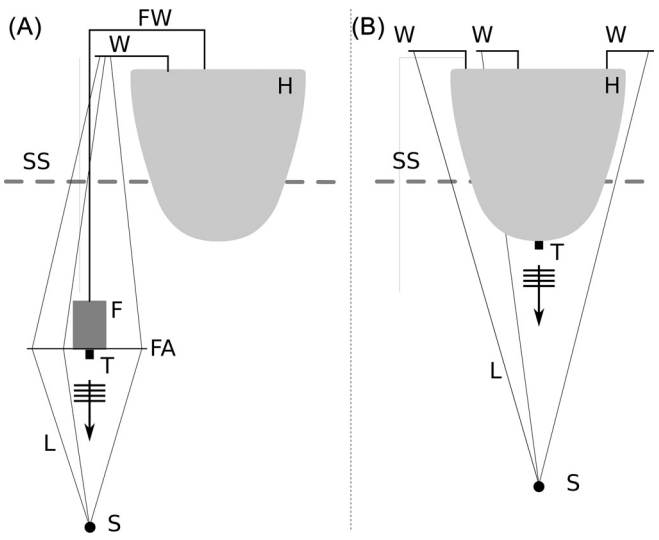

FIG. 1. Experimental apparatus. (A) The frame (F) with attached transducer (T) is lowered from a ship (H) via an opto-electro-mechanical cable and winch (FW) to approximately 10 m deep. The target sphere (S) is suspended below the frame with three monofilament lines (L) that extend from the ship via spreader arms (FA) on the frame to the sphere. The depth of the target sphere below the frame is controlled by adjusting the length of the lines via shipboard winches (W). The sea surface is indicated (SS). (B) The target sphere (S) is suspended below the hull-mounted transducer (T) via three monofilament lines (L), whose length is controlled by three ship-mounted winches (W). The direction of propagation of the transducer-generated acoustic waves are indicated by the downward arrow and crossing perpendicular lines.

The conductivity, temperature, and pressure of the water between the transducer and target were measured before or after the experiments using a conductivity-temperature-depth (CTD) probe.

The following assumptions were made for the experiments:

(a) The echosounder transmit voltage was low enough to prevent nonlinear effects in the transceiver, transducer, and seawater.

(b) Far-field conditions apply, ensuring an incident plane wave and a scattered spherical wave, compatible with the usual definition of TS (ISO, 2017; Morfey, 2000). The minimum transducer to the target range of 10 m was larger than the far-field condition for the 38 kHz, 7° beamwidth transducer [about 8.8 m, given that $r_F = \pi D^2/\lambda$, where D is diameter of the transducer and λ is the wavelength (ISO, 2017)]. At the lowest frequency (38 kHz) and shortest target sphere range (10 m), the kr parameter was approximately 750, satisfying the condition that kr be much larger than one to achieve an incident plane wave. In addition, the largest target sphere diameter was 64 mm, and the 10 m range was larger than the near-field of the scattered wave. Hence, the scattered wave can be treated as a spherical wave.

(c) Variations in acoustic absorption are negligible across the 1 ms duration narrowband pulses (Ainslie, 2010).

(d) The effect of ray-bending was neglected since the maximum off-axis angle was less than 0.2° and the direction of propagation was vertically downward and, hence, nominally perpendicular to typical water density and sound speed stratification.

B. Data processing

For each experiment, the pulse frequency, sphere echo range, amplitude, and angular position of the sphere within

https://doi.org/10.1121/10.0001498

the beam were extracted from the echosounder data and filtered to keep only those echoes within 0.2° of the transducer beam axis. The position of the sphere within the beam was obtained from the split-beam facility of the echosounder, where phase differences in the echo arrival at subarrays of the transducer are used to estimate the arrival angle (Demer *et al.*, 2015). The frequency modulated data were pulse-compressed with a replica of the transmitted pulse and Fourier transformed to give backscatter TS as a function of frequency (Bassett *et al.*, 2018; Chu and Stanton, 1998; Lavery *et al.*, 2017). These data, produced at 30 Hz resolution, were interpolated and specific frequencies selected (38, 120, 180, 190, 200, 210, 220, 300, 320, 328, 333, 338, 340, and 360 kHz) and then treated as narrow-frequency data points for the subsequent processing and analysis. The sound speed profile was calculated from the CTD data (IOC, SCOR, and IAPSO, 2010). Since it was not possible to estimate the functional dependence of the absorption coefficient on temperature, pressure, salinity, and pH *in situ* (Doonan *et al.*, 2003; Francois and Garrison, 1982b, 1982a), the measured absorption coefficients were estimated relative to the predicted values. To do so, consider the sonar equation for a single target

$$\mathrm{EL} = \mathrm{SL} + \mathrm{TS} + 2B - 2\mathrm{TL} - \mathrm{NL}, \tag{1}$$

where EL is the received echo level, SL is the source level, TS is the target strength of the target, B is the one-way beampattern of the transducer (Demer *et al.*, 2015; Simmonds and MacLennan, 2005), TL is the one-way transmission loss, and NL is the noise level. Rearranging to solve for TS, replacing TL with terms for spreading and absorption, assuming that NL is insignificant, and recognizing that SL can be considered as a system gain (G_{sys}) results in

$$\mathrm{TS} = \mathrm{EL} + 2\alpha R + 40\ \log_{10} R - G_{\mathrm{sys}} - 2B(\theta, \varphi), \tag{2}$$

where α is the mean acoustic absorption between the transducer and target, R is the distance from the transducer to the target, and $B(\theta, \varphi)$ is a function of the angular direction (θ, φ) and used to compensate for the angular location of the target within the acoustic beam. This compensation utilizes a beam shape model that was fitted to measurements taken during the calibration (Demer *et al.*, 2015). The mean absorption is then replaced by an integration over the range between the transducer and target and the dependence of some terms on the frequency made explicit:

$$\begin{aligned}\mathrm{TS}_m(f,R) = {} & \mathrm{EL}(f) + 2\int_0^R \alpha_{\mathrm{F\&G}}(f, T(r), S(r), P(r), pH)\, dr \\ & + 40\log_{10} R - G_{\mathrm{sys}}(f) - 2B(f,\theta,\varphi),\end{aligned} \tag{3}$$

where $\mathrm{TS}_m(f, r)$ is the measured TS at frequency f of a target at range R from the transducer, $\alpha_{\mathrm{F\&G}}$ is the absorption coefficient given by Francois and Garrison (1982b, 1982a), which is a function of frequency, temperature (T), salinity (S), and pressure (P) at range r. G_{sys} is the system gain obtained from a calibration exercise, and $B(f, \theta, \varphi)$ is the one-way beampattern of the transducer as a function of frequency and position in the acoustic beam. If f is kept constant, the target is on or very close to the beam axis of the transducer (i.e., $\theta = \phi = 0$) and R is accurately estimated, then as R varies, $\mathrm{TS}_m(f, R)$ should remain constant if the absorption estimate is correct. If not, any trend in $\mathrm{TS}_m(f, R)$ with R reflects the inaccuracy in seawater absorption predicted using the formulas proposed by Francois and Garrison, thus,

$$\begin{aligned}\langle \Delta\alpha \rangle &= \frac{\mathrm{TS}_m(f,R) - \mathrm{TS}_{theo}(f)}{2R} = \frac{d\mathrm{TS}_m(f,R)}{2R} \\ &\approx \frac{\Delta \mathrm{TS}_m(f,R)}{2R}\end{aligned} \tag{4}$$

where $\mathrm{TS}_{theo}(f)$ is the theoretical TS of the sphere (MacLennan, 1981) and $\langle \Delta\alpha \rangle$ is the average excess absorption at frequency f. The division by two in Eq. (4) accounts for the two-way measurement (backscatter). In practise, the mean $\Delta \mathrm{TS}_m$ at each sphere range for each experiment was fit with a linear regression against the range halved to yield $\langle \Delta\alpha \rangle$. Since $\mathrm{TS}_m(f, R)$ is the absorption-corrected TS, a negative $\langle \Delta\alpha \rangle$ indicates that the absorption coefficient calculated from the formulas given by Francois and Garrison (1982b, 1982a) is too low.

C. Estimation of SNR

The SNR was estimated at each sphere range and frequency. Three vertically stacked echo-integration regions, each with a height of 2 m and at least 30 pings duration, were defined. The center region included the sphere echo with the other two immediately above and below the center region. The nautical area scattering coefficient, s_A (MacLennan *et al.*, 2002), was calculated for each region and the effective SNR was then estimated as the dB ratio between the echo energy in the sphere layer (s_{As}) and the average of the echo energy in the two adjacent layers (s_{At} and s_{Ab}),

$$\mathrm{SNR} = 10\ \log_{10}\left[\frac{2s_{As}}{(s_{At} + s_{Ab})}\right]. \tag{5}$$

We note that this definition of SNR is not the background noise level in the ocean, nor the echosounder system noise, but rather a measure of the reverberation level.

III. RESULTS

The experiments were carried out in depth ranges above the dominant thermocline (about 90 m) in regions of slowly varying depth-dependent water properties (Fig. 2). In each experiment, the sphere TS deviated from the theoretical as the range increased (for example, the 2013 narrowband measurements; Fig. 3) as was expected when the estimated absorption is incorrect. The ping-to-ping variability in individual sphere measurements for a given range varied with

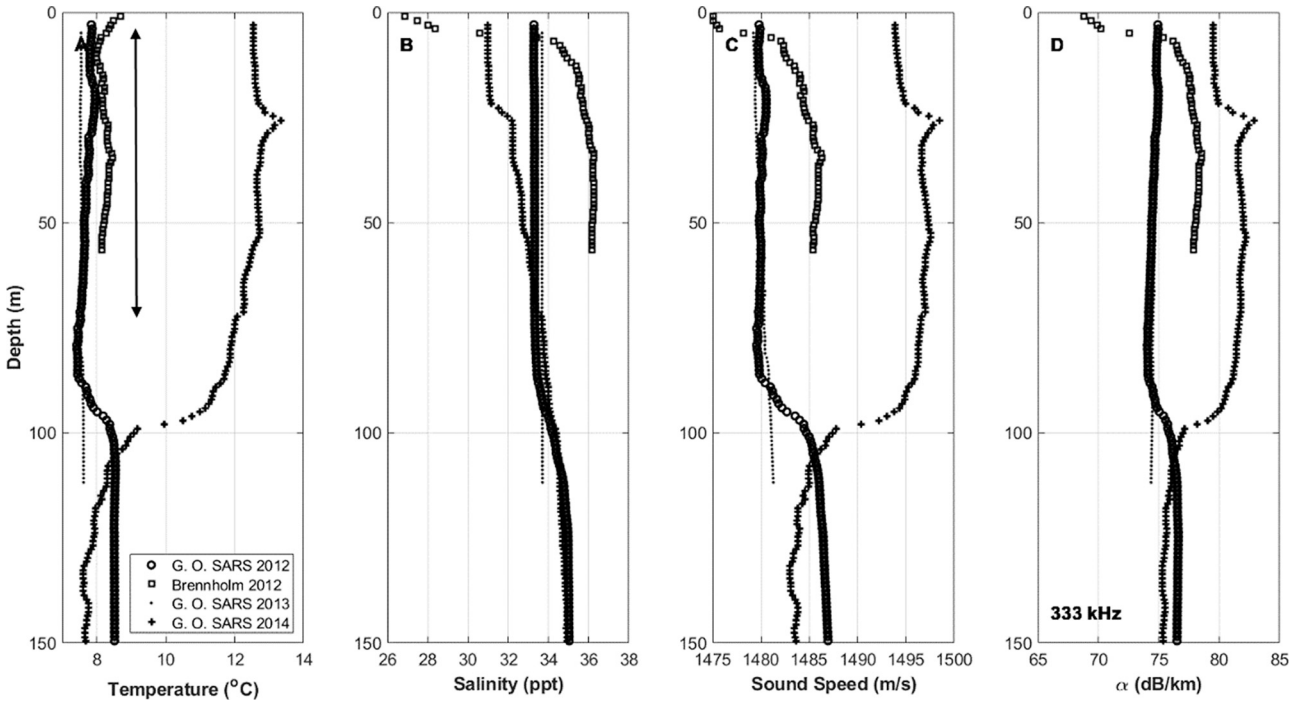

FIG. 2. Temperature (A), salinity (B), and sound speed (C) profiles obtained during the experiments. (D) Estimated absorption at 333 kHz using the Francois and Garrison equations (1982b, 1982a) at the measured temperature, salinity, and depths. The depth range that the target sphere covered is indicated in (A).

frequency and was largest (±1.5 dB) around 333 kHz, decreasing to about ±0.5 dB at 120 kHz (Fig. 3).

For frequencies of 200 kHz or lower, the excess absorption estimates were less than ±4 dB km^{-1} [Fig. 4(A)] with the mean at each frequency being in the range ±1.3 dB km^{-1} (Table II). The standard deviation of the $\langle \Delta\alpha \rangle$ estimates was about ±2 dB km^{-1} (except for 70 kHz, where only one measurement was available), which we interpret as the measurement accuracy of the method and experimental setup. Above 300 kHz, $\langle \Delta\alpha \rangle$ was significantly different from zero (for the 2013 data, p-value = 0.0001) with a mean overall measurement of about −15 dB km^{-1} at 333 kHz [Fig. 4(A)]. The deviation of the measurements above 300 kHz, compared to those calculated using existing equations, are more clearly appreciated when viewed against the absolute absorption curves [Fig. 4(B)].

The SNR decreased with increasing range to the sphere (Fig. 5). The variability with range, apart from the general trend, reflects different densities of weak backscattering at different depths below the sea surface and, additionally, for 38 kHz the presence of weak second bottom echoes. The larger ping-to-ping variability in sphere TS at 333 kHz (Fig. 3) was a consequence of the lower SNR at that frequency.

The rule of thumb that at least 10 dB SNR is required for reliable measurement of a target sphere then suggests that the 333 kHz data are limited to about the 55 m range, whereas the lower frequencies can be used beyond 60 m.

IV. DISCUSSION

The results at 200 kHz and lower are consistent with the Francois and Garrison absorption equations. The large difference in $\langle \Delta\alpha \rangle$ around 333 kHz indicates that the Francois and Garrison equation is incorrect for some input parameters.

The measurements were taken from a restricted set of water properties (Fig. 2) at shallow depths, and the results are not necessarily applicable to other water properties. However, they do raise concerns that the commonly used absorption relationship is sufficiently in error around 333 kHz to cause mistakes in frequency-response-based allocation of acoustic backscatter to species categories. No measurements of excess absorption were obtained between 220 kHz and 300 kHz. However, from the data around 200 kHz and between 300 and 360 kHz, a logarithmic trend in $\langle \Delta\alpha \rangle$ is indicated for the frequency range of 200–360 kHz (Fig. 4).

The overall measurement uncertainty from the experiments includes data variability due to uncertainties in environmental parameters (phytoplankton blooms and microbubbles) and measurement errors due to imprecisions and inaccuracies in the instruments (echosounders, CTD, etc.). The ±2 dB measurement variability is similar to that obtained from earlier measurements (Francois and Garrison, 1982b, 1982a, and references therein).

Acoustic absorption is affected by oceanic phytoplankton spring blooms, which can modify seawater viscosity to the extent that changes in absorption can be observed (Rhodes, 2008). This additional absorption is about 1 dB km^{-1} at 60 kHz and increases to about 20 dB km^{-1} at 333 kHz. However, none of the measurements were obtained during a spring bloom so this type of absorption will not be present in the data. Suspended sediment can also modify seawater viscosity and have a material effect on absorption

https://doi.org/10.1121/10.0001498

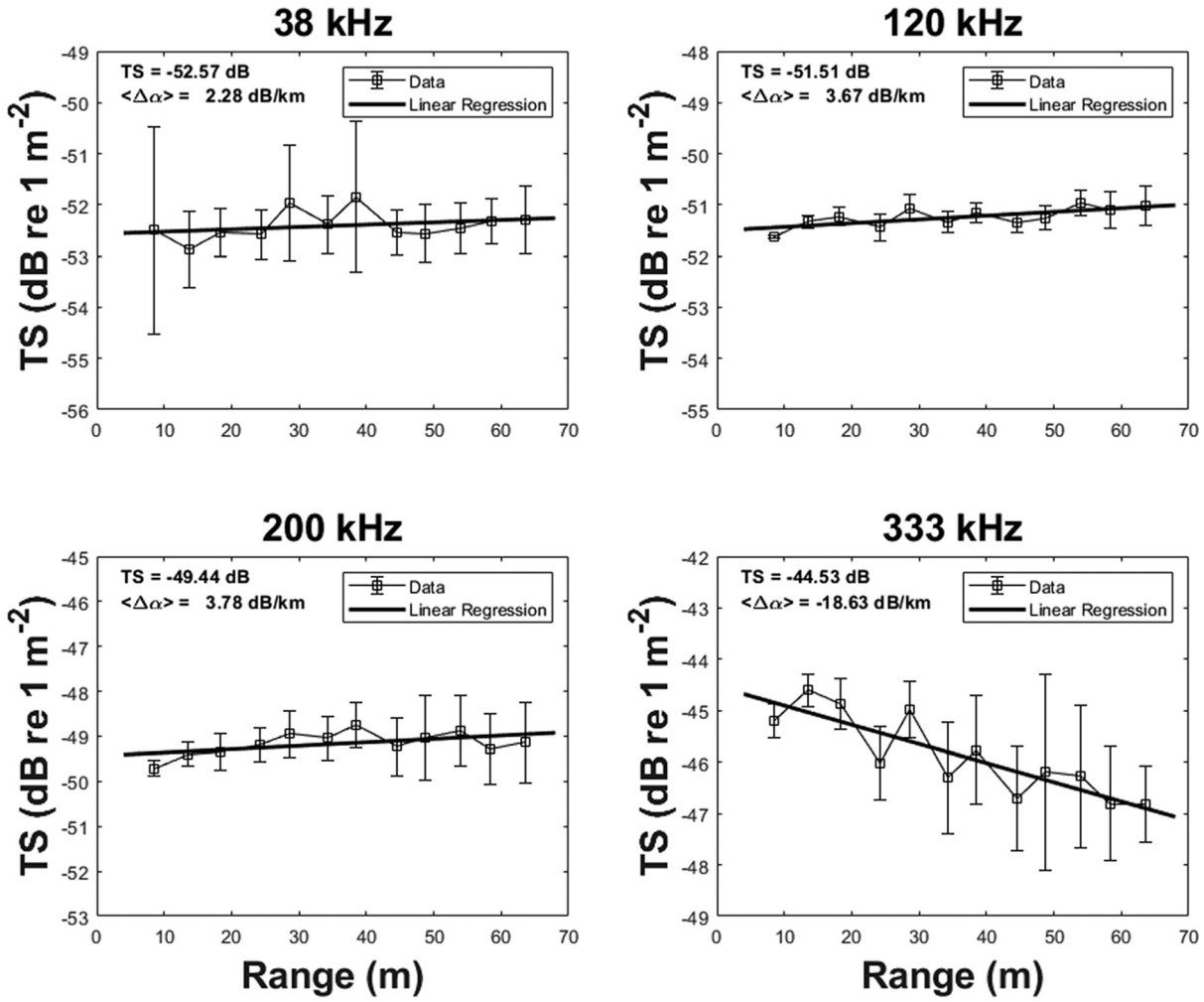

FIG. 3. Sphere TS example from the 2013 experiment at 38, 120, 200, and 333 kHz. The open squares are the measured sphere TS, the vertical lines show the standard deviation of the TS from multiple measurements at each range, and the solid line is a linear regression whose slope is an estimate of the averaged excess seawater absorption between the transducer and the target sphere relative to that estimated by Francois and Garrison (1982b, 1982a). The relevant theoretically derived sphere TSs at 0 m depth are shown on each plot (dB re 1 m^2) as is the slope of the linear regression line (dB km^{-1}).

(Liu *et al.*, 2009). This requires very high levels of sediment that were not present during the experiments. Consequently, neither of these effects will have affected the results.

Another concern is the presence of microbubbles, which can cause additional absorption when the acoustic frequency is similar to the resonance frequency of the bubbles and the numerical density is high (Medwin and Clay, 1998). There was no generation of bubbles from breaking waves at the time of the measurements (Table I), the measurement depth was between 10 and 70 m so the bubble population can be expected to be typical of shallow calm coastal waters (Medwin, 1970; Randolph *et al.*, 2014), and, hence, any absorption due to bubbles can be regarded as an ever-present contribution to the total absorption. In addition, given that at frequencies of 200 kHz and lower, the absorption coefficients were consistent with previously published values but were significantly different around 333 kHz indicates that the effects of the microbubbles were negligible. For example, small microbubbles of 20 μm diameter at 35 m depth would have a resonance frequency of about 150 kHz (Medwin and Clay, 1998) and, therefore, would cause the measured TSs at 120 and 200 kHz to deviate from the predicted TSs, but this was not observed.

At the typical water conditions present during our measurements (temperature of 7 °C, salinity of 33 PSU, and pressure equivalent to a depth of 10 m; Fig. 2), the absorption components at 333 kHz, as calculated from the Francois and Garrison equations (Francois and Garrison, 1982a), are 0.1 dB km^{-1} from boric acid, 36.7 dB km^{-1} from magnesium sulphate, and 39.0 dB km^{-1} from pure water. Since the boric acid component is only significant below about 10 kHz, it is the magnesium sulphate and pure water components in which the differences to our measurements would be expected to occur. The method presented in this paper does not have the ability to indicate which of these is likely to be the cause of the difference, but the form of the relationship used to estimate the magnesium relaxation frequency underestimates the absorption at frequencies above about 200 kHz (Fig. 9 of Francois and Garrison, 1982b). This is consistent with our measurements, suggesting that the magnesium sulphate term may be the main source of the observed difference. In addition, our work at frequencies

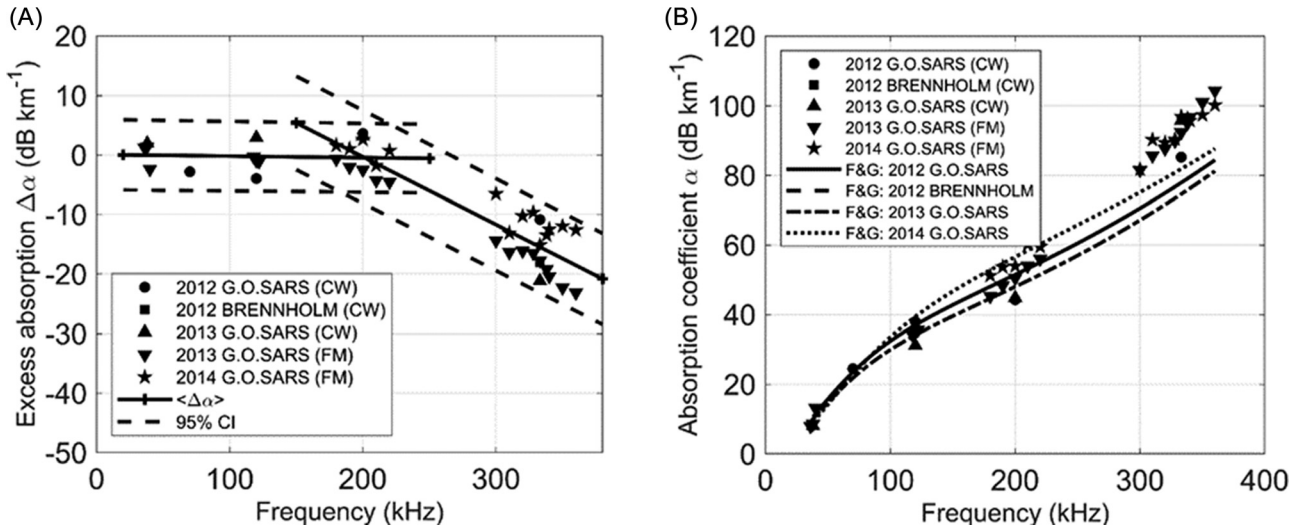

FIG. 4. (A) Excess absorption, $\langle\Delta\alpha\rangle$, relative to that obtained from the Francois and Garrison (1982b, 1982a) formulas for all experiments. The experiments were conducted from RV G. O. Sars and RV Brennholm; FM (frequency modulation) indicates data derived from a broadband pulse and CW (continuous wave) indicates a narrow-frequency pulse. Negative values indicate that the Francois and Garrison absorption estimate is too low. (B) Estimated absolute absorption coefficients with Francois and Garrison (1982b, 1982a) curves drawn for comparison. The Francois and Garrison 2012 Brennholm curve is obscured by the Francois and Garrison 2012 G. O Sars curve.

around 333 kHz comprise 20 measurements from 4 different locations over a 3-year period, all of which gave similar results, lending weight to their validity. The results at lower frequencies where $\langle\Delta\alpha\rangle$ was close to zero also supports the conclusion that the radar pulse method is reliable and the difference around 333 kHz is real.

The use of echosounders to estimate acoustic absorption appears to have not been reported previously. The absorption estimation method described in this paper uses the same equipment and a procedure very similar to that used to calibrate the amplitude response of ship-mounted echosounders (Demer *et al.*, 2015). Hence, the *in situ* measurement of acoustic absorption could be readily carried out during fisheries acoustics surveys.

The method used here has more discriminating power at higher frequencies because for a given range the total absorption is larger and, thus, the ability to detect a change is increased. However, the practical sphere range for this method was found to be approximately 70 m—as the range increased, the SNR decreased (Fig. 5), causing an increased variability in the split-beam position estimates (Kieser *et al.*, 2005) and a corresponding increase in the variability of the sphere TS estimates (Fig. 3). The split beam angular measurements worked well if the SNR was above about 10 dB, and it was clear that with the small target spheres used for the 333 kHz system (TS = −44 dB re 1 m^2), this limit was reached at about 60 m range. At lower frequencies, changes in total absorption between 10 and 70 m become more difficult to reliably measure, given the low total absorption compared to the ping-to-ping variability. It is expected that the maximum practical sphere range could be extended by using a target with a higher TS (i.e., larger diameter) and deploying the measurement system into deeper water with less background scatter (such as can be found in some calm deep fjords). This would reduce the measurement variability and increase the ability to estimate absorption at all frequencies.

The measurements indicate that the existing absorption equations have an increasing error at frequencies above 200 kHz that at 333 kHz produces an estimate that is 15 dB

TABLE II. Estimated seawater absorption error, $\langle\Delta\alpha\rangle$, estimated from the experiments at five commonly used fisheries acoustic survey frequencies, measured between 2012 and 2014. Negative values of $\langle\Delta\alpha\rangle$ indicate that the values estimated from existing equations are too low.

Frequency (kHz)	38	70	120	200	333
$\langle\Delta\alpha\rangle$ (dB km^{-1})	−0.73	0.62	1.31	−1.21	−15.24
Standard deviation of $\langle\Delta\alpha\rangle$(dB km^{-1})	1.98	—	2.45	1.65	2.34

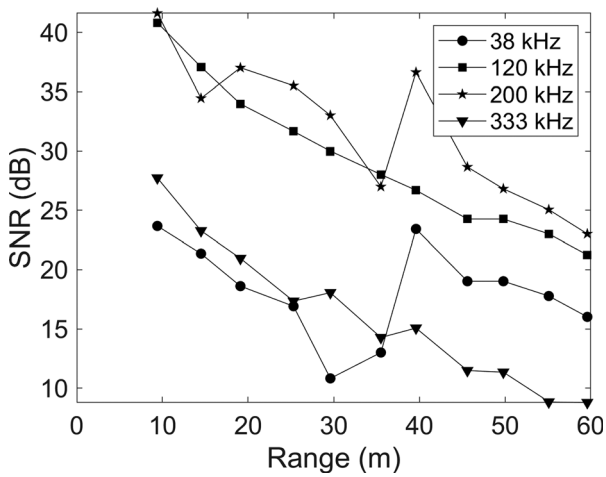

FIG. 5. Estimates of the SNR for the 2013 measurements at 38, 120, 200, and 333 kHz narrowband sphere measurements as a function of range to the sphere. The target sphere diameter was 21.0 mm. Deviations from the general reduction in SNR were caused by depth-dependent scattering layers.

km^{-1} too low. Quantitative use of backscatter at 333 kHz is common in the fisheries acoustics field, and the results emphasise the need for an improved acoustic absorption equation. This could be achieved with additional measurements and reanalysis of existing measurements.

ACKNOWLEDGMENTS

This work was carried out with support from the Norwegian Research Council through the Centre for Research-Based Innovation in Sustainable Fish Capture and Processing Technology and the WESTZOO project (Exploiting new wideband echosounder technology for zooplankton characterization, sizing, and abundance estimation). The authors thank Ronald Pedersen for his assistance with the experiments.

Ainslie, M. (**2010**). *Principles of Sonar Performance Modelling*, 1st ed. (Springer-Verlag, Berlin, Heidelberg), 828 pp.
Ainslie, M. A., and McColm, J. G. (**1998**). "A simplified formula for viscous and chemical absorption in sea water," J. Acoust. Soc. Am. **103**, 1671–1672.
Bassett, C., De Robertis, A., and Wilson, C. D. (**2018**). "Broadband echosounder measurements of the frequency response of fishes and euphausiids in the Gulf of Alaska," ICES J. Mar. Sci. **75**, 1131–1142.
Chu, D., and Stanton, T. (**1998**). "Application of pulse compression techniques to broadband acoustic scattering by live individual zooplankton," J. Acoust. Soc. Am. **104**, 39–55.
Demer, D. A., Berger, L., Bernasconi, M., Bethke E., Boswell, K., Chu, D., Domokos, R., Dunford, A. J., Fässler, S. M. M., Gauthier, S., Hufnagle, L. T., Jech, J. M., Bouffant, N., Lebourges-Dhaussy, A., Lurton, X., Macaulay, G. J., Perrot, Y., Ryan, T. E., Parker-Stetter, S., Stienessen, S., Weber, T. C., and Williamson, N. J. (**2015**). "Calibration of acoustic instruments," ICES Cooperative Research Report No. 326, p. 130.
Doonan, I., Coombs, R., and McClatchie, S. (**2003**). "The absorption of sound in seawater in relation to estimation of deep-water fish biomass," ICES J. Mar. Sci. **60**, 1047–1055.
Fisher, F. H., and Simmonds, V. P. (**1977**). "Sound absorption in seawater," J. Acoust. Soc. Am. **62**, 558–564.
Francois, R. E., and Garrison, G. R. (**1982a**). "Sound absorption based on ocean measurements. Part II: Boric acid contribution and equation for total absorption," J. Acoust. Soc. Am. **72**, 1879–1890.
Francois, R. E., and Garrison, G. R. (**1982b**). "Sound absorption based on ocean measurements. Part I: Pure water and magnesium sulphate contributions," J. Acoust. Soc. Am. **72**, 896–907.
IOC, SCOR, and IAPSO (**2010**). "The international thermodynamic equation of seawater—2010: Calculation and use of thermodynamic properties," Intergovernmental Oceanographic Commission, Manuals and Guides No. 56, UNESCO, p. 156.
ISO 18405:2017 (**2017**). "Underwater acoustics—Terminology" (International Organization for Standardization, Geneva, Switzerland).
Kieser, R., Reynisson, P., and Mulligan, T. J. (**2005**). "Definition of signal-to-noise ratio and its critical role in split-beam measurements," ICES J. Mar. Sci. **62**, 123–130.
Korneliussen, R., and Johnsen, E. (**2015**) (personal communication).
Korneliussen, R. J., Heggelund, Y., Eliassen, I. K., and Johansen, G. O. (**2009**). "Acoustic species identification of schooling fish," ICES J. Mar. Sci. **66**, 1111–1118.
Krautkrämer, J., and Krautkrämer, H. (**1990**). "The pulse-echo method; Design and performance of a pulse-echo flaw detector," in *Ultrasonic Testing of Materials* (Springer, Berlin), pp. 167–221.
Kurtze, G., and Tamm, K. (**1953**). "Measurements of sound absorption in water and in aqueous solutions of electrolytes," Acta Acust. Acust. **3**, 33–48.
Lavery, A. C., Bassett, C., Lawson, G. L., and Jech, J. M. (**2017**). "Exploiting signal processing approaches for broadband echosounders," ICES J. Mar. Sci. **74**, 2262–2275.
Liebermann, L. N. (**1948**). "The origin of sound absorption in water and in sea water," J. Acoust. Soc. Am. **20**, 868–873.
Liu, Y., Li, Q., and Chen, M. (**2009**). "The experimental investigation on measuring sound absorption in the seawater containing suspended sediment particles," in *9th International Conference on Electronic Measurement and Instruments (ICEMI)* (IEEE), Vol. 4, pp. 616–621.
MacLennan, D. N. (**1981**). "The Theory of Solid Spheres as Sonar Calibration Targets," Scottish Fisheries Research Report No. 22, Department of Agriculture and Fisheries for Scotland, p. 17.
MacLennan, D. N., Fernandes, P., and Dalen, J. (**2002**). "A consistent approach to definitions and symbols in fisheries acoustics," ICES J. Mar. Sci. **59**, 365–369.
Medwin, H. (**1970**). "*In situ* acoustic measurements of bubble populations in coastal ocean waters," J. Geophys. Res. **75**, 599–611, https://doi.org/10.1029/JC075i003p00599.
Medwin, H., and Clay, C. S. (**1998**). "Fundamentals of acoustical oceanography," in *Applications of Modern Acoustics* (Academic, Boston), 712 pp.
Morfey, C. (**2000**). *The Dictionary of Acoustics*, 1st ed. (Academic, San Diego), 430 pp.
Ochi, H., Watanabe, Y., Shimura, T., and Hattori, T. (**2009**). "Measurement of absorption coefficients at 80 kHz band for broadband underwater acoustic data transmission," in *ICCAS-SICE 2009*, IEEE, pp. 2364–2367.
Pinkerton, J. M. M. (**1947**). "A pulse method for the measurement of ultrasonic absorption in liquids: Results for water," Nature **160**, 128–129.
Randolph, K., Dierssen, H. M., Twardowski, M., Cifuentes-Lorenzen, A., and Zappa, C. J. (**2014**). "Optical measurements of small deeply penetrating bubble populations generated by breaking waves in the Southern Ocean," J. Geophys. Res.: Oceans **119**, 757–776, https://doi.org/10.1002/2013JC009227.
Rhodes, C. J. (**2008**). "Excess acoustic absorption attributable to the biological modification of seawater viscosity," ICES J. Mar. Sci. **65**, 1747–1750.
Simmonds, J., and MacLennan, D. (**2005**). *Fisheries Acoustics. Theory and Practice*, 2nd ed. (Blackwell Science, Oxford), 437 pp.
van Moll, C. A. M., Ainslie, M. A., and van Vossen, R. (**2009**). "A simple and accurate formula for the absorption of sound in seawater," IEEE J. Ocean. Eng. **34**, 610–616.